Power Quality Disturbance Localization Using Maximal Overlap Discrete Wavelet Transform

Swarnabala Upadhyaya* and Sanjeeb Mohanty†
Department of Electrical Engineering
National Institute of Technology Rourkela, Rourkela-769 008, India
*swarnabala.u@gmail.com †sanjeeb.mohanty@nitrkl.ac.in

***Abstract*—In recent times, the wavelet-based methodologies have been developed as suitable alternatives for the real-time analysis of power system. In this paper the time-series based maximal overlap discrete wavelet transform (MODWT) technique has been proposed for the detection and the localization of different PQ disturbances. The performance of the MODWT has been compared with the traditional discrete wavelet transform (DWT). Ten different types of PQ disturbances of the voltage signal such as sag, swell, interruption, harmonic, sag with harmonics and swell with harmonics, spike, notch etc. are analyzed with the two different types of wavelet transform (WT). Each signal is decomposed up to fourth level by applying both the DWT and the MODWT. However, the MODWT is appropriate for the real-time detection of PQ disturbances as it has an ability for the free selection of the initial point of the time series. Similarly, MODWT is can apply on signal of any sample size.**

***Index Terms*—Power quality disturbance, wavelet transform, maximal overlap discrete wavelet transform, discrete wavelet transform**

[1]

I. Introduction

All over the world, the power quality (PQ) has become a pressing concern due to the continuous increasing of the number of distributing loads in industries as well as in the public sectors. The presence of disturbances in the loads makes the deviation of voltage and current from the ideal waveform that declines the performance and the lifespan of the equipments [1]. Moreover, the electrical disturbance signals are treated as one of the similar time series data. The sudden decrease and increase of voltage signal are identified as sag and swell, respectively. If the frequency becomes an integer multiple of the fundamental frequency then the harmonics are generated. But when the electronically controlled capacitor switched on, transient type disturbances are found and similarly multiple integral frequency known as harmonics, notch are also observed in solid state power electronics circuits. Besides these disturbances, spike is also generated due to the lightening, and the arc furnace operation lead to flicker. In order to mitigate these disturbances, the signal patterns like sag, swell, interruption etc. must be distinguished first. As a result, the automated classification of the disturbances has become a significant issue in deregulated power system where the PQ is becoming one of the important discriminating factors for choosing different suppliers [2]. However, the existing automatic recognition methods for time series pattern need enhancement with the efficiency and reliability.

In order to identify the type of power signal waveforms, several authors has introduced different methodology such as the fast operated Fourier transform (FT), the short-time Fourier transform (STFT), the wavelet transform (WT), the Neural Network, the Fuzzy logic, the S-transform [3], [4], [5], [6], [7], [8] and [9]. The commonly used STFT is only suitable for steady state disturbances like sag and swell but the transient signals including notch cannot be analysed due to the fixed window [10], [11] and [12]. Heisenberg-Gabor inequality [13] limits the time-frequency resolution of the signals in STFT analysis. The WT based on multi resolution analysis (MRA) is extensively used for non-stationary signal characterisation that provides the time-frequency relationship by convolving the dilated and translated wavelet with signal.

The automatic detection of PQ events with the discrete wavelet transform (DWT) is a common topic in past studies [14], [15]. But the DWT is restricted with the size of the signal. A modified version of DWT is known as maximal overlap discrete wavelet transform (MODWT) is adopted in this paper. The coefficients of the proposed method are not affected by changing the starting point and also has no restrictions on the size of signal unlike the traditional DWT. The MODWT has been implemented [16], [17] as 'undecimated DWT' with the context of infinite sequence. Similarly, MODWT is implemented as 'translation invariant DWT' [18], [19] and 'time-invariant DWT' [20].

The paper is organised as follows. Section II describes the brief theory of the DWT and MODWT for carrying out the process of detection. The PQ disturbance model is given in Section III. In Section IV, the effectiveness of DWT and MODWT is presented to detect different PQ disturbances. Finally the Section-V, concludes the paper.

II. Wavelet Transform

The presentation of the signal as a combination of small wavelets at different location (amplitude or position) and scales (time or duration) is known as Wavelet Transform (WT). The transformation process from the time domain to time-scale domain known as signal decomposition or signal analysis which is a forward process and similarly the reverse process called the inverse wavelet transform or signal reconstruction.

[1]978-1-4673-6540-6/15/$31.00 2015 IEEE

A. *Discrete Wavelet Transform*

The DWT is one of the useful techniques used to decompose a discretized signal into different resolution levels. In DWT decomposition, the wavelet function generates the detailed coefficients of the decomposed signal whereas the scaling function generates the approximation coefficients of the decomposed signal. The expression for DWT with $g(\cdot)$ as the mother wavelet is given as [21]

$$DWT(m,k) = \frac{1}{\sqrt{a_0^m}} \sum_n x(n) g\left(\frac{k - nb_0a_0^m}{a_0^m}\right) \tag{1}$$

where k is an integer that is used to refer the sample, scaling parameter and translation parameter. Both a and b vary in the discrete manner. At the first level of decomposition, the time signal is decomposed into detailed as well as the smooth part through the high pass $h(n)$ and low pass filters $l(n)$. Thus, the detail version contains high-frequency components than the smooth version. Mathematically, they are specified as

$$c_1(n) = \sum_k h(k-2n)c_0(k) \tag{2}$$

$$d_1(n) = \sum_k g(k-2n)c_0(k) \tag{3}$$

The discretized time signal is (sampled version of) of the original signal. After each decomposition, the number of samples are reduced to half as the output is down sampled by a factor 2. The approximation coefficients are then further fed to the low pass and the high pass filter to iterate the process. The low pass and low pass filters are called as the 'Quadrature mirror filters' which are related by the equation (13)

$$h[L-1-n] = (-1)^n l(n) \tag{4}$$

where, L is the filter length. The signal is fed to both the low pass and high pass filter as shown in Fig. 1. The implementation of DWT is restricted with the length of signals. Similarly, the coefficients are affected by the change of initial point. The MODWT has been implemented in order to overcome the sensitivity of DWT with the choice of starting point of a time series.

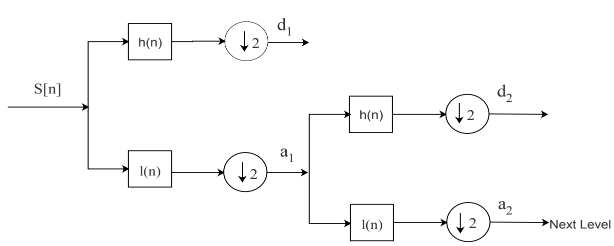

Fig. 1. Block diagram representation of DWT decomposition

B. *Maximum Overlapping Discrete Wavelet Transform (MODWT)*

The primary motivation to formulate MODWT over the traditional DWT is the flexibility of selection of the starting point of a time series signal. The sensitivity to the initial choice point has reduced by the elimination of down sampling. The MODWT is the modified version of the DWT which can be employed to any sample size, unlike the DWT. The implementation of DWT is limited by sample size of multiple of $2s$. The MODWT can be implemented to any segment N to be an inter multiple of 2^j for $j = 1, 2, 3, \ldots, J$ is the scale and J is the level of MODWT decomposition [14], [15]. The basic block diagram of MODWT is shown in Fig. 2. The MODWT scaling filter $\widetilde{h}_l$ and the wavelet filters $\widetilde{g}_l$ are equivalent to the DWT filters through (5) and (6)

$$\widetilde{h}_l = \frac{h_l}{\sqrt{2}} \tag{5}$$

$$\widetilde{g}_l = \frac{g_l}{\sqrt{2}}. \tag{6}$$

The quadrature mirrors are also used like DWT filter is presented as (8) and (7)

$$\widetilde{g}_l = (-1)^{l+1} h_{L-1-l} \tag{7}$$

$$\widetilde{h}_l = (-1)^{l+1} g_{L-1-l} \tag{8}$$

where $l = 0, 1, 2, \ldots, L-1$ and L is the width of the filter. The n^{th} element of the first-stage wavelet and the scaling coefficients of MODWT with the input time series signal $X(n)$ is presented as (9) and (10)

$$\widetilde{W}_{1,n} = \sum_{l=0}^{L_1-1} \widetilde{h}_l X_{n-l \mod N} \tag{9}$$

$$\widetilde{V}_{1,n} = \sum_{l=0}^{L_1-1} \widetilde{g}_l X_{n-l \mod N} \tag{10}$$

where $n = 1, 2, 3, \ldots, N$ and N is the length of signal in sample.

$$\widetilde{A}_{1,n} = \sum_{l=0}^{L_1-1} \widetilde{g}_l \widetilde{V}_{1,n+l \mod N} \tag{11}$$

$$\widetilde{D}_{1,n} = \sum_{l=0}^{L_1-1} \widetilde{g}_l \widetilde{W}_{1,n+l \mod N}. \tag{12}$$

The first-stage approximations and details can be calculated from the equations (11) and (12). The MODWT scaling coefficients $\widetilde{V}_j$ and $\widetilde{W}_j$ wavelet coefficients at the n^{th} element of the j^{th} stage are given by the equations (13) and (14) as

$$\widetilde{V}_{j,n} = \sum_{l=0}^{L_j-1} \widetilde{g}_{j,1} \widetilde{X}_{n-l \mod N} \tag{13}$$

$$\widetilde{W}_{j,n} = \sum_{l=0}^{L_j-1} \widetilde{h}_{j,1} \widetilde{X}_{n-l \mod N} \tag{14}$$

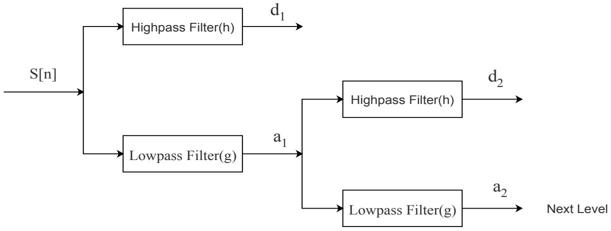

Fig. 2. Block diagram representation of MODWT decomposition

Similarly, the approximations $\widetilde{A}_j$ and the details $\widetilde{D}_j$ of the n^{th} element of the j^{th} stage MODWT are given by the equations (15) and (16) as

$$\widetilde{A}_{j,n} = \sum_{l=0}^{L_j-1} \widetilde{g}^0_{j,l}\widetilde{V}_{1,n+l} \mod N \tag{15}$$

$$\widetilde{D}_{j,n} = \sum_{l=0}^{L_j-1} \widetilde{h}^0_{j,l}\widetilde{W}_{1,n+l} \mod N \tag{16}$$

where $\widetilde{g}^0_l$ is periodized $\widetilde{g}$ to length N and also the $\widetilde{h}^0_l$ is periodized $\widetilde{h}$ to length N. So the original time series signal can be expressed in terms of the approximations and the details as (17)

$$X(n) = \sum_{l=0}^{j} \widetilde{D}_j + \widetilde{A}_j. \tag{17}$$

The original signal can be regained easily from the decomposed signals like the traditional DWT and FT techniques. The DWT and proposed MODWT has been implemented in the subsequent Section.

III. Power Quality Disturbance Model

The PQ analysis comprises of both the stationary and non-stationary signals such as the voltage swell, sag, interruption, spike, harmonic with sag and so on. In this paper, ten types of different disturbances along with the pure sine wave are considered for analysis. These PQ disturbances are analysed with ten cycles of a waveform of 50 Hz fundamental frequency. The sampling frequency is 3.2 KHz. The signals are simulated according to the model [22] and [23].

IV. Results and Discussion

The PQ disturbances presented in Table I are fed as inputs to Fig. 1 and Fig. 2. Moreover, ten types of power quality disturbances along with the normal sinusoidal voltage are decomposed up to fourth levels using both DWT and MODWT.

A. Pure Sinusoidal Wave

A pure sinusoidal wave of voltage signal is considered in Fig.3. With DWT and MODWT, the signal is decomposed up to four decomposition levels are shown in Fig.3 along with the original sine wave. The the vertical axis represents the amplitude of voltage signal in volt V p.u. (per unit) and similaly the horizontal axis presents the time (in second) in terms of samples. Both DWT and MODWT are implemented on the aforementioned PQ signals in order to carry out the analysis.

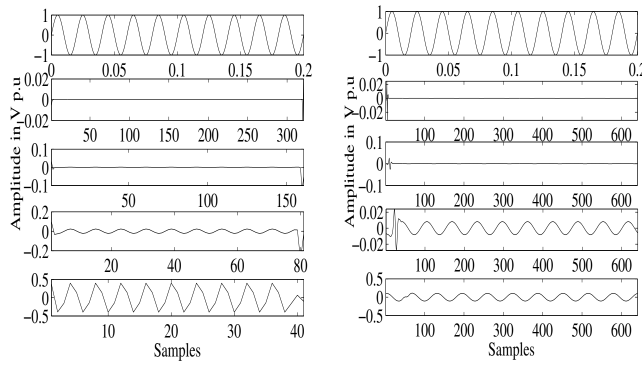

(a) (b)

Fig. 3. Localization of pure sine wave in (a) DWT decomposition (b) SGWT decomposition

By decomposing normal voltage, similar types of waveforms are produced at the respective decomposition level both in DWT and the MODWT present in Fig. 3 along with the original waveform. In MODWT, the initial point is shifted due to circular shifting which helps in future prediction.

B. Pure Sinusoidal Wave with Sag

A pure sine wave signal with sag is analysed in Fig. 4. The four finer decomposition levels of the DWT and the MODWT decomposition along with the original signal waveform are shown in Fig. 4. The first decomposition level of each of the technique shows the exact time of occurrence of the sag. The inception point of sag is shifted along with the initial point of signal towards right due to circular shift. The shifting property of MODWT assists the prediction further inception.

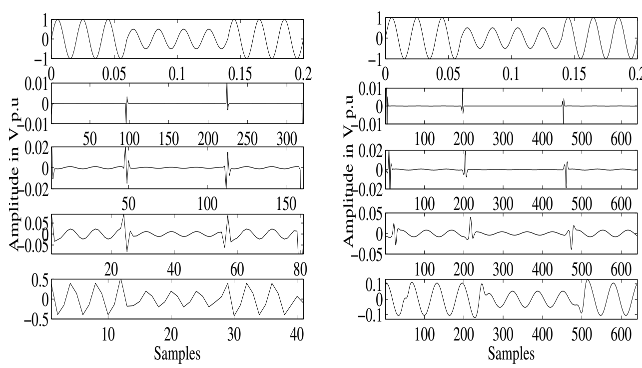

(a) (b)

Fig. 4. Localization of pure sine wave in (a) DWT decomposition (b) SGWT decomposition

C. Pure Sinusoidal Wave With Swell

Similarly, the swell in pure sine wave is detected and localized in the decomposed levels using both DWT and MODWT in Fig. 5. The point of occurrence of the swell

TABLE I
POWER QUALITY DISTURBANCE MODELS

PQD events	Equations
Normal Voltage	$h(t) = \sin(\omega t)$
Sag	$h(t) = [1 - \alpha(u(t - t_1) - u(t - t_2))] \sin(\omega t)$
Swell	$h(t) = [1 + \alpha(u(t - t_1) - u(t - t_2))] \sin(\omega t)$
Interruption	$h(t) = [1 - \alpha(u(t - t_1) - u(t - t_2))] \sin(\omega t)$
Oscillatory transient	$h(t) = \sin(\omega t) + \alpha \exp(-(t - t_1)\tau)(u(t - t_1) - u(t - t_2)) \sin(2\pi f_n t)$
Harmonics	$h(t) = \alpha_1 \sin(\omega t) + \alpha_3 \sin(3\omega t) + \alpha_5 \sin(5\omega t) + \alpha_7 \sin(7\omega t)$
Sag + Harmonics	$h(t) = [1 - \alpha(u(t - t_1) - u(t - t_2))] (\alpha_1 \sin(\omega t) + \alpha_3 \sin(3\omega t) + \alpha_5 \sin(5\omega t))$
Swell + Harmonics	$h(t) = [1 + \alpha(u(t - t_1) - u(t - t_2))] (\alpha_1 \sin(\omega t) + \alpha_3 \sin(3\omega t) + \alpha_5 \sin(5\omega t))$
Notch	$h(t) = \sin(\omega t) - \text{sign}(\sin(\omega t)) \left\{ \sum_{k=0}^{9} k[u(t - (t_1 + 0.2n)) - u(t - (t_1 + 0.2n))] \right\}$
Spike	$h(t) = \sin(\omega t) + \text{sign}(\sin(\omega t)) \left\{ \sum_{k=0}^{9} k[u(t - (t_1 + 0.2n)) - u(t - (t_1 + 0.2n))] \right\}$
Flicker	$h(t) = [1 + \alpha \sin(2\pi\beta t)] \sin(\omega t)$

and also the duration can be easily identified at first level decomposition in both the cases. The time series analysis of MODWT has given the idea for the further prediction of swell in the subsequent decomposition levels. Moreover, the MODWT provides estimation of disturbance location, which helps in the power system relaying.

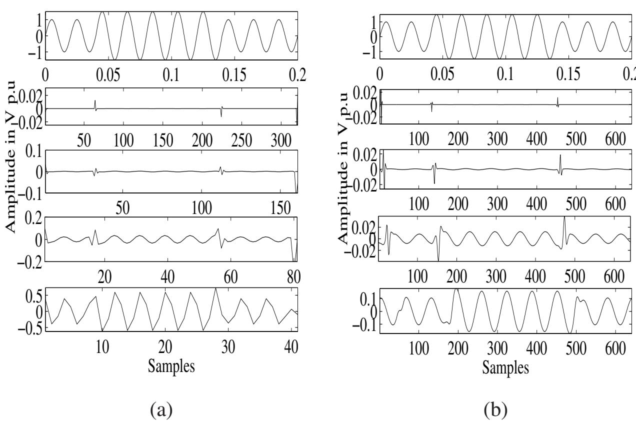

Fig. 5. Localization of sine wave with swell in (a) DWT decomposition (b) MODWT decomposition

D. Pure Sinusoidal Wave with Interruption

The interruption in pure sine wave is localized and detected at the first decomposition of both MODWT and DWT. The point of interruption is prominently identified in both MODWT and DWT decompositions. The interruption is detected and localized at each decomposition levels in both the cases given in the Fig. 6. One-step-ahead predictions property of MODWT leads us to the arrival of the onset timing of further interruption in the signal. This one step ahead prediction is suitable for relaying.

E. Pure Sinusoidal Wave With Notch

The pure sine wave with the notch at each cycle is considered for analysis. The notches are precisely localized at the decomposition levels of DWT and MODWT in Fig. 7. The MODWT and DWT waveform has provided localization of notch.

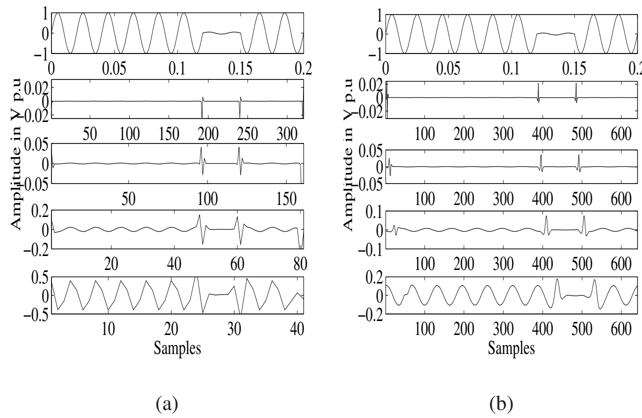

Fig. 6. Localization of sine wave with interruption in (a) DWT decomposition (b) MODWT decomposition

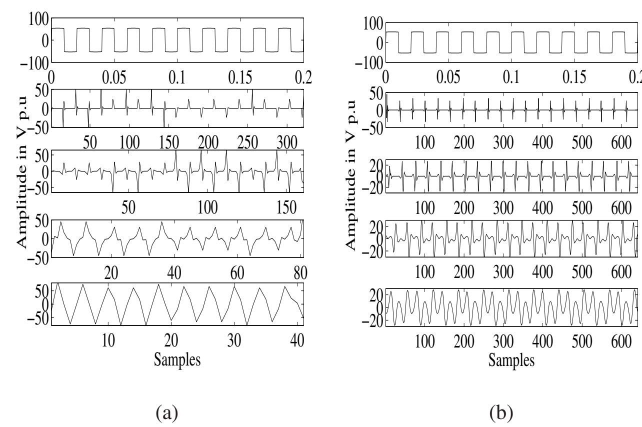

Fig. 7. Localization of sine wave with notch in (a) DWT decomposition (b) SGWT decomposition

F. Pure Sinusoidal Wave With Oscillatory Transients

The transient oscillatory signal is analyzed in Fig. 8 with both DWT and MODWT decompositions. The signal is analysed using both the DWT and MODWT up to four levels as shown in Fig. 8.The signal retains original property MODWT, as there is no down sampling. The elimination of down sampling in MODWT, eliminate the restriction with the size of signal i.e., any length signal can be analyzed unlike the DWT.

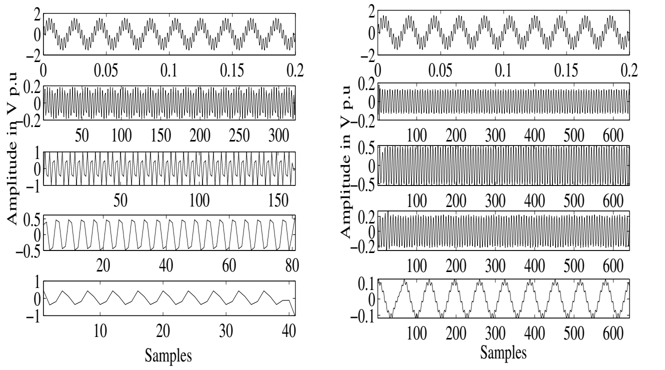

(a) (b)

Fig. 8. Localization of sine wave with oscillatory transient in (a) DWT decomposition (b) MODWT decomposition

G. Pure Sinusoidal Wave With Flicker

The flicker signal is considered for analysis in Fig. 9. The detection and the localization of flicker are accomplished using traditional DWT and shifting based MODWT decomposition and are given in Fig. 9. The MODWT has provided proper localization of flicker at all levels of decomposition like DWT.

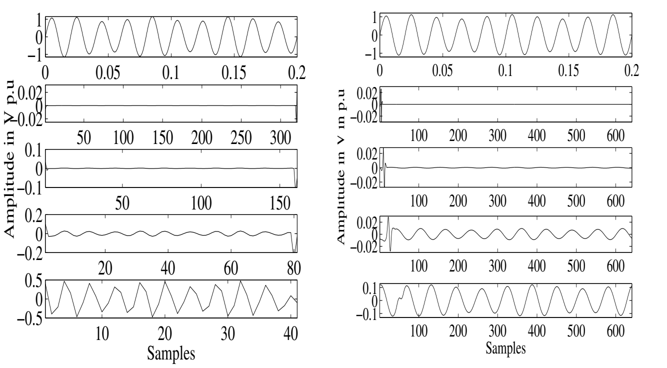

(a) (b)

Fig. 9. Localization of sine wave with flicker in (a) DWT decomposition (b) MODWT decomposition

H. Pure Sinusoidal Wave With Spike

Similar to the notch signal, the spike at each cycle of pure sine wave is also considered for analysis. The localization of spike is done satisfactorily with both DWT and MODWT as shown in Fig. 10.

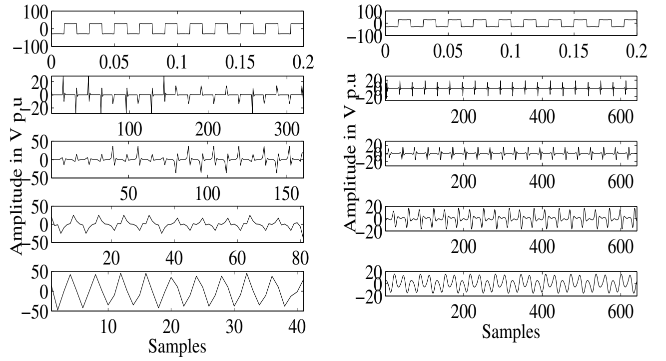

(a) (b)

Fig. 10. Localization of sine wave with spike in (a) DWT decomposition (b) MODWT decomposition

I. Pure Sinusoidal Wave With Harmonics

The harmonics with fundamental is analysed in Fig. 11 with DWT and MODWT. From the Figs. 11 and 3, it can be seen that for sinusoidal signal the magnitude of 1^{st} two levels are almost zero and for harmonic signal, 1^{st} two levels have some magnitude both in DWT and MODWT.

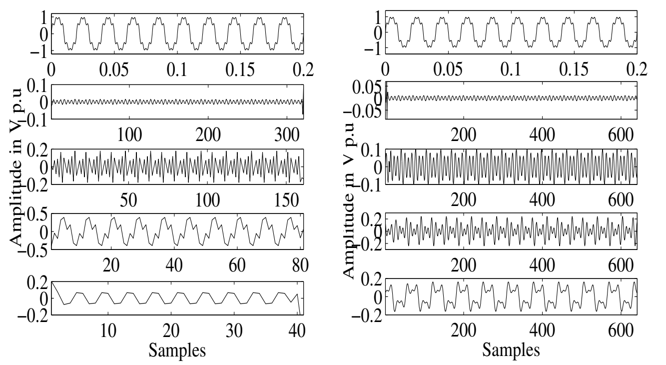

(a) (b)

Fig. 11. Localization of sine wave with harmonics in (a) DWT decomposition (b) MODWT decomposition

J. Pure Sinusoidal Wave With Sag and Harmonics

The distortions of a pure sine wave due the sag and harmonic are localized in the decomposition levels of DWT and MODWT as shown in Fig. 12.

K. Pure Sinusoidal Wave With Swell and Harmonics

Similarly, the swell with harmonic signal is considered for analysis. The swell with harmonic is detected and localized at the decomposition levels of DWT and MODWT decomposition as shown in Fig.13.

The aforementioned PQ signals are simulated with a core-i5,2.40 GHz under MATLAB environment. Though both the DWT and MODWT use a low-pass filter and a high-pass filter (quadrature mirror filter) to split the frequency band of these aforementioned input signals in order to get scaling

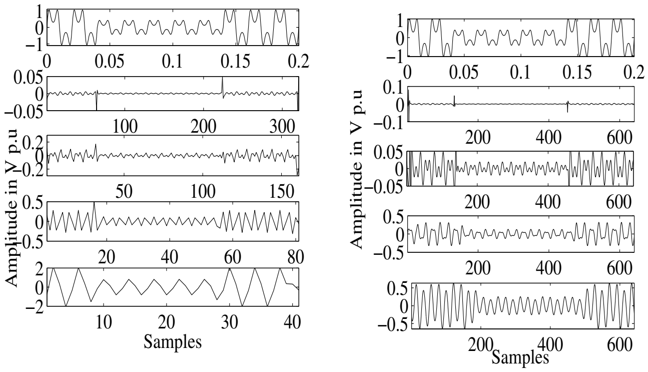

(a) (b)

Fig. 12. Localization of sine wave with sag and harmonics in (a) DWT decomposition (b) MODWT decomposition

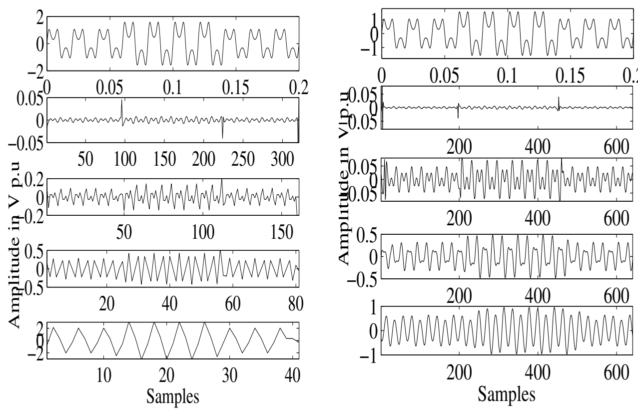

(a) (b)

Fig. 13. Localization of sine wave with swell and harmonic in (a) DWT decomposition (b) MODWT decomposition

and wavelet coefficients, respectively, but there is no down sampling in MODWT unlike in DWT. The time-invariant transformation property of MODWT has increased its application for any length of the signal with the context of DWT.

V. Conclusion

The Wavelet Transform is a significant tool for the analysis in PQ environment disturbances. The convolution based DWT and the time series based MODWT have been used to localize the PQDs. Ten types of PQ disturbances along with the sinusoidal voltage signal wave form are properly analysed with the proposed MODWT. The down sampling free MODWT provides the proper localization of PQDs along with the shifting. Elimination of down sampling overcomes the restriction in the choice of signal length. The insensitivity to the choice of starting point of time series turns MODWT as a suitable tool in real time environment.

References

[1] M. Valtierra-Rodriguez, R. de Jesus Romero-Troncoso, R. A. Osornio-Rios, and A. Garcia-Perez, "Detection and classification of single and combined power quality disturbances using neural networks," *Industrial Electronics, IEEE Transactions on*, vol. 61, no. 5, pp. 2473–2482, 2014.

[2] T. Abdel-Galil, E. El-Saadany, A. Youssef, and M. Salama, "Disturbance classification using hidden markov models and vector quantization," *Power Delivery, IEEE Transactions on*, vol. 20, no. 3, pp. 2129–2135, 2005.

[3] L. Coppola, Q. Liu, S. Buso, D. Boroyevich, and A. Bell, "Wavelet transform as an alternative to the short-time fourier transform for the study of conducted noise in power electronics," *Industrial Electronics, IEEE Transactions on*, vol. 55, no. 2, pp. 880–887, 2008.

[4] Z.-L. Gaing, "Wavelet-based neural network for power disturbance recognition and classification," *Power Delivery, IEEE Transactions on*, vol. 19, no. 4, pp. 1560–1568, 2004.

[5] J. G. Decanini, M. S. Tonelli-Neto, F. C. Malange, and C. R. Minussi, "Detection and classification of voltage disturbances using a fuzzy-artmap-wavelet network," *Electric Power Systems Research*, vol. 81, no. 12, pp. 2057–2065, 2011.

[6] J. Barros, M. de Apraiz, and R. I. Diego, "A virtual measurement instrument for electrical power quality analysis using wavelets," *Measurement*, vol. 42, no. 2, pp. 298–307, 2009.

[7] C. Bhende, S. Mishra, and B. Panigrahi, "Detection and classification of power quality disturbances using s-transform and modular neural network," *Electric Power Systems Research*, vol. 78, no. 1, pp. 122–128, 2008.

[8] T. Nguyen and Y. Liao, "Power quality disturbance classification utilizing s-transform and binary feature matrix method," *Electric Power Systems Research*, vol. 79, no. 4, pp. 569–575, 2009.

[9] M. Uyar, S. Yildirim, and M. T. Gencoglu, "An expert system based on s-transform and neural network for automatic classification of power quality disturbances," *Expert Systems with Applications*, vol. 36, no. 3, pp. 5962–5975, 2009.

[10] A. A. Abdelsalam, A. A. Eldesouky, and A. A. Sallam, "Characterization of power quality disturbances using hybrid technique of linear kalman filter and fuzzy-expert system," *Electric power systems Research*, vol. 83, no. 1, pp. 41–50, 2012.

[11] A. Gaouda, M. Salama, M. Sultan, A. Chikhani, *et al.*, "Power quality detection and classification using wavelet-multiresolution signal decomposition," *IEEE Transactions on Power Delivery*, vol. 14, no. 4, pp. 1469–1476, 1999.

[12] L. Angrisani, P. Daponte, M. Apuzzo, and A. Testa, "A measurement method based on the wavelet transform for power quality analysis," *Power Delivery, IEEE Transactions on*, vol. 13, no. 4, pp. 990–998, 1998.

[13] B. Biswal and S. Mishra, "Power signal disturbance identification and classification using a modified frequency slice wavelet transform," *Generation, Transmission & Distribution, IET*, vol. 8, no. 2, pp. 353–362, 2014.

[14] A. G. Hafez, E. Ghamry, H. Yayama, and K. Yumoto, "A wavelet spectral analysis technique for automatic detection of geomagnetic sudden commencements," *Geoscience and Remote Sensing, IEEE Transactions on*, vol. 50, no. 11, pp. 4503–4512, 2012.

[15] D. B. Percival and A. T. Walden, "Wavelet methods for time series analysis (cambridge series in statistical and probabilistic mathematics)," 2000.

[16] M. J. Shensa, "The discrete wavelet transform: wedding the a trous and mallat algorithms," *Signal Processing, IEEE Transactions on*, vol. 40, no. 10, pp. 2464–2482, 1992.

[17] G. P. Nason and B. W. Silverman, "The stationary wavelet transform and some statistical applications," *LECTURE NOTES IN STATISTICS-NEW YORK-SPRINGER VERLAG-*, pp. 281–281, 1995.

[18] R. Coifman and D. Donoho, "Translation-invariant de-noising, in wavelets and statistics(a. antoniadis, ed.)," 1995.

[19] R. Coifman and D. Donoho, "Translation-invariant de-noising, in wavelets and statistics(a. antoniadis, ed.)," 1995.

[20] J.-C. Pesquet, H. Krim, and H. Carfantan, "Time-invariant orthonormal wavelet representations," *Signal Processing, IEEE Transactions on*, vol. 44, no. 8, pp. 1964–1970, 1996.

[21] K. C. Hwan and R. Aggarwal, "Wavelet transform in power systems: Part 1 general introduction to the wavelet transform," *IEE–Power Engineering Journal*, vol. 14, no. 2, pp. 81–87, 2000.

[22] C.-Y. Lee and Y.-X. Shen, "Optimal feature selection for power-quality disturbances classification," *Power Delivery, IEEE Transactions on*, vol. 26, no. 4, pp. 2342–2351, 2011.

[23] S. Upadhyaya and S. Mohanty, "Power quality disturbance detection using wavelet based signal processing," in *India Conference (INDICON), 2013 Annual IEEE*, pp. 1–6, IEEE, 2013.